arXiv:1510.00169v1 [cond-mat.stat-mech] 1 Oct 2015

Functional renormalization group approach to non-collinear magnets

B. Delamotte,[1,*] M. Dudka,[2,†] D. Mouhanna,[1,‡] and S. Yabunaka[3,§]

[1] *Sorbonne Universités, UPMC Univ Paris 06, LPTMC, CNRS UMR 7600, F-75005, Paris, France*
[2] *Institute for Condensed Matter Physics, National Acad. Sci. of Ukraine, UA–79011 Lviv, Ukraine*
[3] *Yukawa Institute for Theoretical Physics, Kyoto University, Kyoto 606-8502, Japan*

A functional renormalization group approach to d-dimensional, N-component, non-collinear magnets is performed using various truncations of the effective action relevant to study their long distance behavior. With help of these truncations we study the existence of a stable fixed point for dimensions between $d = 2.8$ and $d = 4$ for various values of N focusing on the critical value, $N_c(d)$, that, for a given dimension d, separates a first order region for $N < N_c(d)$ from a second order region for $N > N_c(d)$. Our approach concludes to the *absence* of stable fixed point in the physical – $N = 2, 3$ and $d = 3$ – cases, in agreement with $\epsilon = 4 - d$-expansion and in contradiction with previous perturbative approaches performed at fixed dimension and with recent approaches based on conformal bootstrap program.

PACS numbers: 75.10.Hk, 11.10.Hi, 12.38.Cy

I. INTRODUCTION

Non-collinear – or canted – XY or Heisenberg magnets are one of the simplest examples of physical systems for which the order parameter is not a *vector*, as in the collinear case, but a $2nd$-order tensor, that is, a *matrix* [1]. As a consequence, the rotation group is fully broken in the low temperature phase. This is particularly clear for the stacked triangular antiferromagnetic (STA) spin system, since, in the ground state, the spins on a plaquette exhibit the famous 120° structure which *completely* breaks the $SO(N)$ rotation group with $N = 2$ or 3. This change of symmetry-breaking pattern between collinear and non-collinear magnets alters drastically the critical physics which is not yet fully clarified despite forty years of intensive research (see [1] and references therein).

On the experimental side there is agreement that at the phase transition, both XY and Heisenberg non-collinear magnets exhibit scaling laws but with critical exponents differing from those of the $O(N)$ model. This has lead to two kinds of scenarios: either the phase transitions belong to a new universality class [2] or they are *weakly* of first order [1]. A careful analysis of the results coming from different materials shows that the critical exponents vary from one compound to the other and there is in fact no universality [1]. This tends to confirm the assumption of weak first order transitions as do almost all numerical simulations performed on STA or on similar models [3–11] but one [12]. However all these results do not rule out definitively the possibility that some other systems undergo a second order phase transition.

On the theoretical side, all approaches agree that in the vicinity of four dimensions, there exists a line $N_c(d)$ in the (d, N) plane above which the transition is of second order and below which it is of first order. At two loops, $N_c(d = 4 - \epsilon) = 21.8 - 23.4\epsilon + O(\epsilon^2)$ [13, 14], which shows that perturbative corrections are large and that it is therefore impossible to extrapolate reliably this result in $d = 3$ without computing the contributions of higher orders. The perturbative calculation of $N_c(d)$ either within the ϵ or pseudo-ϵ-expansion [13–19] or directly in $d = 3$ [12, 20–23] has been performed up to five or six loops. The same quantity has also been computed within the nonperturbative renormalization group (NPRG) approach [1, 24–30].

However the various results so far obtained do not agree in particular in the physically interesting $N = 2$ and $N = 3$ cases. On the one hand, the ϵ and pseudo-ϵ-expansion and the NPRG approach both lead to a value of $N_c(d = 3)$ well above 3. Indeed: $N_c(d = 3) = 6.1(6)$ within the ϵ-expansion at five loops [18], $N_c(d = 3) = 6.22(12)$ [18] and $N_c(d = 3) = 6.23(21)$ [19] within the pseudo-ϵ-expansion at six loops and finally $N_c(d = 3) = 5.1$ within the NPRG approach [1]. Moreover the NPRG approach predicts that the transitions are weakly of first order for $N = 2$ and 3, accompanied by a non-universal scaling behavior in agreement with both numerical computations and experiments. On the other hand, perturbative computations performed at fixed dimension lead to completely different predictions [12, 22, 23]. Those performed at six loops within the zero momentum massive scheme [23] lead to two different $N_c(d = 3)$: N_{c1} and N_{c2}. Above $N_{c1} = 6.4(4)$ there are, as usual, two fixed points, one stable and one unstable. They get closer when N is lowered, collide at N_{c1} and disappear. However, below $N_{c2} = 5.7(3)$, a stable fixed point reappears and exists for $N = 2$ and 3. A second order phase transition is therefore predicted for these values of N. A puzzling feature of this fixed-dimension computation is that it predicts, in the (d, N) plane, a curve $N_c(d)$ showing a very unusual S-like shape around $d = 3$ or, equivalently, a *non-monotonic* curve $d_c(N)$, the dimension below which, for a given N the transi-

*Electronic address: delamotte@lptmc.jussieu.fr
†Electronic address: maxdudka@icmp.lviv.ua
‡Electronic address: mouhanna@lptmc.jussieu.fr
§Electronic address: yabunaka@scphys.kyoto-u.ac.jp

tion is of second order. If true, this would imply that at $d = 3$, a second order transition occurs for low values of N whereas at larger values it would be of first order before being *again* of second order. As for computations performed at five loops within the minimal subtraction ($\overline{MS}$) scheme *without* ϵ-expansion [12], no critical value of N is found in $d = 3$ and, thus, a second order phase transition is predicted for *any* value of N.

In order to solve the contradiction between the different approaches, a careful re-analysis of the resummation procedures used within fixed-dimension calculations has been performed in [31–33]. Some very peculiar features have been revealed by this analysis: lack of convergence of the critical quantities with the order of the expansion, high sensitivity of the results with respect to the resummation parameters, existence of the non-trivial fixed point *at* and *above* the upper critical dimension $d = 4$, etc. This re-analysis have cast grave doubts upon the reliability of the fixed-dimension approaches when applied to non-collinear magnets.

From the results above, it is tempting to believe that a coherent picture of the critical behavior of non-collinear magnets has been reached and that the transitions are of (weak) first order whereas fixed-dimensions approaches would be not converged or deficient. However, recently, a new approach, based on the conformal bootstrap (CB) program (see for instance [34] and references therein), has been applied to $O(N)\times O(M)$ models [35, 36], the $M = 2$ case corresponding to non-collinear magnets. This program when applied to other systems such as the three-dimensional ferromagnetic Ising model [37, 38] leads to the best determination of the critical exponents ever obtained. It also has the advantage of being *a priori* unbiased by convergence problems since it is not based on series expansions, contrary to RG methods. As for the $O(N) \times O(M)$ models, the authors of [36] have found with the CB approach a stable fixed point for $N = 3$ and $M = 2$ in $d = 3$ with critical exponents in good agreement with the fixed-dimension perturbative results and thus in disagreement with both the ϵ, pseudo-ϵ-expansion and NPRG results. However, it is important to notice two points. First, the CB program assumes scale invariance, that is, the existence of a second order phase transition which is precisely the main question addressed in the context of non-collinear magnets. Second, in all RG-based schemes, there exists, in the RG flow diagram, either two nontrivial fixed points or none. Indeed the very mechanism that determines the curve $N_c(d)$ when N is lowered keeping d fixed is the collapse of the stable – chiral – fixed point C_+ controlling the phase transition with another unstable – anti-chiral – fixed point C_-. However, this fixed point C_- is not found within the CB analysis of the $O(3) \times O(2)$ model [36], which contrasts with the other approaches.

The results obtained within the CB program have led us to re-examine the NPRG approach to non-collinear magnets, looking for possible failures in previous computations [1, 24–30] that were based on two kinds of approximation: (i) the derivative expansion of the action at its lowest order, called the local potential approximation (LPA) [24–26]; (ii) a field expansion of the effective action including the effects of derivative terms at leading order [1, 27–30].

In this article, we go beyond these approximations by performing: (i) an approximation – called field-semi-expansion – where the most important field-dependence is considered without approximation, *i.e.* functionally, the remainder being approximated using a field-expansion; (ii) an approximation where no field-expansion at all is performed. Moreover in these two approximations the most important derivative terms are taken into account at leading order. The results of our analysis corroborate all conclusions reached within previous NPRG approaches in particular for the value of $N_c(d = 3)$ that we find to be significantly larger than 3. They thus disagree with those obtained with the fixed-dimension perturbative approaches as well as with the CB program.

The article is organized as follow. In section II, we briefly recall the principle and properties of the NPRG approach that we use. In section III, we present the effective action relevant for non-collinear magnets within this approach. We discuss in particular its symmetries, the symmetry breaking scheme and, finally, the approximations used. In section IV, we present the NPRG equations for non-collinear magnets. In section V, we give the results obtained under the form a field-semi-expansion of the associated effective potential. In section VI, we discuss the results obtained using a full functional approximation of the effective action where only the derivative terms are truncated. In section VII, we conclude.

II. THE EFFECTIVE ACTION METHOD

The central object of the NPRG approach is a running effective action – or Gibbs free energy – Γ_k [39, 40] that includes the statistical fluctuations between the typical microscopic momentum scale Λ of the system – the inverse of a lattice spacing for instance – down to the running scale $k < \Lambda$. In the limit $k \to \Lambda$, no fluctuation is taken into account and $\Gamma_{k=\Lambda}$ identifies with the classical action – or microscopic Hamiltonian – while when $k \to 0$, all fluctuations are summed over and the usual Gibbs free energy Γ is recovered:

$$\begin{cases} \Gamma_{k=\Lambda} = S \\ \\ \Gamma_{k=0} = \Gamma \ . \end{cases} \tag{1}$$

Thus, at any finite scale $k < \Lambda$, Γ_k interpolates between the action and the Gibbs free energy. To construct the running effective action, the original partition function :

$$\mathcal{Z}[J] = \int D\zeta \exp\Big(- S[\zeta] + \int_q J(q)\zeta(-q)\Big) \tag{2}$$

where $\int_q = \int d^dq/(2\pi)^d$, is modified by adding a cut-off term to the classical action:

$$\Delta S_k[\zeta] = \frac{1}{2}\int_q R_k(q^2)\ \zeta(q)\zeta(-q) \tag{3}$$

in which $R_k(q^2)$ is a cut-off function that ensures the separation between the low- and high-momentum modes. The k-dependent partition function thus writes:

$$\mathcal{Z}_k[J] = \int D\zeta \exp\left(-S[\zeta] - \Delta S_k[\zeta] + \int_q J(q)\zeta(-q)\right). \tag{4}$$

It is convenient to choose $R_k(q^2)$ such that: (i) it behaves as a mass at low momentum q in order to freeze the low-momentum fluctuations; (ii) it vanishes at large momentum q in order to keep unchanged the high-momentum fluctuations. Thus one has:

$$\begin{cases} R_k(q^2) \sim k^2 & \text{when} \quad q^2 \ll k^2 \\ R_k(q^2) \to 0 & \text{when} \quad q^2 \gg k^2\ . \end{cases} \tag{5}$$

These constraints on $R_k(q^2)$ also imply that $R_{k=0}(q^2) \equiv 0$ which is consistent with the fact that when $k = 0$ all fluctuations have been summed over and the original model is retrieved: $\mathcal{Z}_{k=0}[J] = \mathcal{Z}[J]$. Finally note that $R_{k=\Lambda}(q^2)$ is very large for all momenta much smaller than Λ. A typical cut-off function satisfying all the previous requirements is:

$$R_k(q^2) = \frac{Z_k q^2}{e^{q^2/k^2} - 1} \tag{6}$$

where Z_k is the field renormalization – see below. Another useful cut-off function, called theta cut-off, has been proposed by Litim [41]. It writes:

$$R_k(q^2) = Z_k\left(k^2 - q^2\right)\Theta\left(k^2 - q^2\right) \tag{7}$$

where Θ is the usual step function.

The running Gibbs free energy Γ_k is then defined as the (slightly modified) Legendre transform of the Helmoltz free energy $W_k[J] = \log \mathcal{Z}_k[J]$ (see [1, 42–46]):

$$\Gamma_k[\phi] = -W_k[J] + J.\phi - \Delta S_k[\phi] \tag{8}$$

where ϕ is the order parameter field and where a mass term analogous to (3) has been added with respect to the usual definition of Γ for the following reason. Clearly, since $R_{k=0}(q^2) \equiv 0$, with the definition Eq.(8) one recovers the usual free energy in the limit $k \to 0$: $\Gamma_{k\to 0} = \Gamma$. The limit $k \to \Lambda$ is less trivial since, there, the cut-off function $R_k(q^2)$ is very large. But one can show [1, 42–46] that the cut-off term $\Delta S_k[\phi]$ in Eq.(8) conspires with that included in $W_k[J]$ and makes that $\Gamma_{k=\Lambda}[\phi] \simeq S[\phi]$. One thus recovers the conditions Eqs.(1).

The effective action follows an exact flow equation, the Wetterich equation [47–50]:

$$\partial_t \Gamma_k[\phi] = \frac{1}{2}\mathrm{Tr}\int_q \dot{R}_k(q^2)\left(\Gamma_k^{(2)}[q, -q, \phi] + R_k(q^2)\right)^{-1} \tag{9}$$

where $t = \ln k/\Lambda$ and $\dot{R}_k = \partial_t R_k$. In Eq.(9), Tr must be understood as a trace over internal vector or tensor indices if the order parameter ϕ spans a nontrivial representation of a group which is the case for non-collinear magnets. Finally $\Gamma_k^{(2)}[q, -q, \phi]$ stands for the Fourier transform of the second functional derivative of Γ_k with respect to the order parameter field:

$$\Gamma^{(2)}_{k,i,j}[x, y, \phi] = \frac{\delta\Gamma_k[\phi]}{\delta\phi_i(x)\delta\phi_j(y)} \tag{10}$$

for a N-component field with components ϕ_i. Thus the quantity $(\Gamma_k^{(2)}[\phi] + R_k)^{-1}$ appearing in Eq.(9) represents the *exact*, *i.e.* field-dependent, propagator.

The general properties of Eq.(9) have been discussed at length in the literature [1, 42–46]. We recall only some of them that are directly relevant for our purpose. First, Eq.(9) is exact, notably because the propagator $(\Gamma_k^{(2)}[\phi] + R_k)^{-1}$ is the exact, field-dependent one. As a consequence, Eq.(9) embodies all perturbative and non-perturbative features of the model under study: spin-waves, topological excitations, bound states, tunneling, etc. Second, due to the property of the cut-off function R_k, Eq.(9) is, due to the presence of a "mass-term" R_k in the propagator, infrared finite for any $k > 0$. Also, due to presence of the function $\dot{R}_k$ that rapidly decays for high momenta, *i.e.* $q^2 > k^2$, it is ultraviolet finite. Thus Eq.(9) allows to explore criticality directly in three dimensions without having recourse to tricks like ϵ-expansion techniques for instance. Third, Eq.(9) has a one-loop structure which implies that all integrals encountered are single integrals in contrast with perturbative expansions at high orders that lead to involved multiple integrals. This property makes straightforward comparisons with leading order of *all* perturbative approaches : weak coupling, low temperature, large-N, expansions in their respective domains of validity.

Now, although exact, Eq.(9) must be approximated in order to get concrete results for complicated problems with optimal efforts. This is realized by choosing a truncation for $\Gamma_k[\phi]$. Among the most popular ones one finds, for a scalar field theory:

(i) *Derivative expansion.* Γ_k is expanded in powers of the derivatives of the order parameter:

$$\Gamma_k[\phi] = \int_x \left\{U_k(\phi) + \frac{1}{2}\ Z_k(\phi)\,(\partial\phi)^2 + \mathcal{O}((\partial\phi)^4)\right\} \tag{11}$$

from which one gets *functional* RG equations for the potential part $U_k(\phi)$ and kinetic part $Z_k(\phi)$ of the running effective action by appropriate functional derivations of Eq.(9). The rationale behind this approximation is that when the anomalous dimension is small, gradient terms should play only a small role at long distance and high-order derivative terms should be negligible.

(ii) *Combined derivative and field expansions.* On top of the derivative expansion, the functions $U_k(\phi)$ and $Z_k(\phi)$ are expanded in powers of ϕ around a given field

configuration. This kind of approximation converts the functional equation Eq.(9) into a set of ordinary coupled differential equations for the coefficients of the expansion. This approximation relies on the double assumption that the anomalous dimension is small and that the correlation functions with a high number of legs have a small back-reaction in the RG flow on those with a small number of legs. Neglecting them should therefore not spoil the dominant critical behavior.

(iii) *Field expansion.* Γ_k is expanded in powers of the order parameter ϕ. One has:

$$\Gamma_k[\phi] = \sum_{n=0}^{\infty} \frac{1}{n!} \left(\int_{x_i} \prod_{i=0}^{n} \phi(x_i) \right) \mathcal{V}_k^{(n)}(x_1, ..., x_n) \qquad (12)$$

where $\mathcal{V}_k^{(n)}(x_1, ..., x_n)$ are the vertices of the theory. Applying then Eq.(9) to this expansion allows to generate a hierarchy of RG equations for the vertices. Approximations are then performed on Γ_k in order to close this hierarchy. This kind of approach relies on the assumption that vertices of high orders in the field can be neglected while the full functional dependence with respect to derivatives – or momenta – must be kept. This is very likely not the generic situation.

(iv) *Green function*, also called *Blaizot–Méndez-Galain–Wschebor (BMW)* [51–53], approach. Its aim is to keep the full momentum dependence of the two-point functions and the functional dependence of the potential $U_k(\phi)$ and $Z_k(\phi)$ functions. It consists in approximating the momentum dependence of the three- and four-point functions in the flow of the two-point functions. It thus reproduces the results obtained within the derivative expansion at small momenta while being also non-perturbative at high momenta.

From a practical point of view the main difficulty lies in the choice of approximation that contains the most important features of the model under study while being also technically manageable. For critical phenomena one can focus on momenta q close to 0. The method of choice is therefore the derivative expansion (see (i) above). This is in contrast with situations where bound states – or, more generally, excitations exhibiting a non-trivial momentum structure – are expected in which a more or less important momentum dependence should be considered through the use of (iii) or (iv). At leading order of the derivative expansion one completely neglects the effects of derivative terms and sets the field renormalization function $Z_k(\phi)$ equal to one, keeping a full function $U_k(\phi)$ for the potential part. This is the so-called local potential approximation (LPA). A possible improvement of this approach consists in replacing now $Z_k(\phi)$ by a non-trivial constant Z_k from which follows a k-dependent anomalous dimension $\eta_k = -(1/Z_k)\partial_t Z_k$, the usual anomalous dimension being given by η_k at a fixed point. This approximation is sometimes called the LPA'. This is essentially this approach that is employed in this article. Note for completeness that one can also try to treat the kinetic terms $Z_k(\phi)$ as a function. However, in practice this has only been performed in the simplest case of $O(N)$ models [54]. For more involved models only approximation (ii) has been used. This approach, when used at reasonably high orders in the field-expansion, is in general sufficient to obtain high precision results. For the Ising model for instance, the best estimates of the critical exponents in $d = 3$ have been recovered with this combined derivative and field expansion employed at fourth order in the derivative and tenth order in the field [55].

Finally, let us emphasize that while the accuracy of the results obviously depend on the order of the truncations none of the approximations presented above spoils the nonperturbative character of the method. Indeed, although the effective action itself is approximated, the very structure of Eq.(9) is kept unchanged as far as the left-hand side is not expanded in powers of one of the usual perturbative parameters: coupling constant, temperature, or $1/N$. Thus even at the lowest order of the combined derivative and field-expansion one already gets results unreachable by perturbative methods [1, 42–46].

III. THE EFFECTIVE ACTION FOR NON-COLLINEAR MAGNETS

We now present the derivative expansion of the effective action relevant to non-collinear magnets. First we recall that for N-component non-collinear magnets, the order parameter consists of two N-component real vectors $\vec{\phi}_1$ and $\vec{\phi}_2$ which, in the STA model, represent linear combinations of the spins of a plaquette [1]. It is convenient to gather these two fields into a $N \times 2$ matrix: $\Phi = (\vec{\phi}_1, \vec{\phi}_2)$. In the continuum limit, the action for non-collinear magnets displays a $O(N) \times O(2)$ invariance where $O(N)$ stands for the usual rotational invariance while $O(2)$ reflects the original C_{3v} symmetry of the lattice [1]. The left $O(N)$ and right $O(2)$ transformations are implemented on Φ by:

$$\begin{cases} \Phi \to U\Phi, \ U \in O(N) \\ \\ \Phi \to \Phi V, \ V \in O(2) \ . \end{cases} \qquad (13)$$

As said above the derivative expansion consists in expanding Γ_k in powers of $\partial\phi$ at a finite order. We consider here the expansion at second order in derivatives where Γ_k writes[1]:

$$\Gamma_k[\vec{\phi}_1,\vec{\phi}_2] = \int_x \Big\{ U_k(\rho,\tau) + \frac{1}{2}Z_k(\rho,\tau)\Big(\big(\partial\vec{\phi}_1\big)^2 + \big(\partial\vec{\phi}_2\big)^2\Big) + \frac{1}{4}Y_k^{(1)}(\rho,\tau)\big(\vec{\phi}_1\cdot\partial\vec{\phi}_2 - \vec{\phi}_2\cdot\partial\vec{\phi}_1\big)^2 + \\ + \frac{1}{4}Y_k^{(2)}(\rho,\tau)\big(\vec{\phi}_1\cdot\partial\vec{\phi}_1 + \vec{\phi}_2\cdot\partial\vec{\phi}_2\big)^2 + \frac{1}{4}Y_k^{(3)}(\rho,\tau)\Big(\big(\vec{\phi}_1\cdot\partial\vec{\phi}_1 - \vec{\phi}_2\cdot\partial\vec{\phi}_2\big)^2 + \big(\vec{\phi}_1\cdot\partial\vec{\phi}_2 + \vec{\phi}_2\cdot\partial\vec{\phi}_1\big)^2\Big)\Big\} \ . \tag{14}$$

In Eq.(14), ρ and τ are the two independent $O(N)\times O(2)$ invariants that read in terms of $\vec{\phi}_1$ and $\vec{\phi}_2$:

$$\begin{cases} \rho &= \mathrm{Tr}({}^t\Phi.\Phi) = \vec{\phi}_1^{\,2} + \vec{\phi}_2^{\,2} \\ \tau &= \frac{1}{2}\mathrm{Tr}\left({}^t\Phi.\Phi - \mathbb{1}\ \frac{\rho}{2}\right)^2 \\ &= \frac{1}{4}\Big(\vec{\phi}_1^{\,2} - \vec{\phi}_2^{\,2}\Big)^2 + \big(\vec{\phi}_1\cdot\vec{\phi}_2\big)^2 \ . \end{cases} \tag{15}$$

The term $U_k(\rho,\tau)$ in Eq.(14) represents the potential part of the effective action while $Z_k(\rho,\tau)$ and $Y_k^{(i)}(\rho,\tau)$, $i=1,2,3$, are kinetic parts. At the minimum of the potential $U_k(\rho,\tau)$ the vectors $\vec{\phi}_1$ and $\vec{\phi}_2$ are orthogonal with the same norm, which corresponds to the following configuration:

$$\Phi_0 = \begin{pmatrix} \phi & 0 \\ 0 & \phi \\ 0 & 0 \\ \vdots & \vdots \\ 0 & 0 \end{pmatrix} \tag{16}$$

where ϕ is a constant. For the spins on the lattice, the configuration Eq.(16) corresponds to the 120° structure. Notice that τ has been built such that it vanishes in this configuration. The ground state Eq.(16) is invariant under the $O(N-2)$ group of left rotations and a diagonal $O(2)$ group – $O(2)_{\mathrm{diag}}$ – that combines left and right rotations:

$$\begin{pmatrix} O(2) & 0 \\ 0 & O(N-2) \end{pmatrix} \Phi_0\ O(2) = \Phi_0 \ . \tag{17}$$

The symmetry breaking scheme is thus given by: $O(N)\times O(2) \to O(N-2)\times O(2)_{\mathrm{diag}}$. For $N=3$ one recovers the symmetry breaking scheme:

$$G = O(3)\times O(2) \to H = \mathbb{Z}_2 \times O(2)_{\mathrm{diag}} \tag{18}$$

which shows that the order parameter space is given by $SO(3)$. For $N=2$ the symmetry breaking scheme is given by:

$$G = O(2)\times O(2) \to H = O(2)_{\mathrm{diag}} \tag{19}$$

or simply by $SO(2)\times\mathbb{Z}_2 \to \mathbb{1}$ where the degrees of freedom associated with the $\mathbb{Z}_2$ group are referred to as chirality excitations.

We now proceed to further approximations. As explained in [1], only the functions Z_k and $Y_k^{(1)}$ contribute to the physics of Goldstone modes and thus are supposed to be the most relevant at the transition. Thus we consider the following simplified effective action:

$$\Gamma_k = \int_x \Big\{ U_k(\rho,\tau) + \frac{1}{2}Z_k(\rho,\tau)\Big(\big(\partial\vec{\phi}_1\big)^2 + \big(\partial\vec{\phi}_2\big)^2\Big) + \frac{1}{4}Y_k^{(1)}(\rho,\tau)\big(\vec{\phi}_1\cdot\partial\vec{\phi}_2 - \vec{\phi}_2\cdot\partial\vec{\phi}_1\big)^2\Big\} \ . \tag{20}$$

A last approximation consists in neglecting the field-dependence of the functions $Z_k(\rho,\tau)$ and $Y_k^{(1)}(\rho,\tau)$ and, thus, in setting $Z_k(\rho,\tau) = Z_k$ and $Y_k^{(1)}(\rho,\tau) = \omega_k$. This approximation has been used in [1, 27–30] in which the function $U_k(\rho,\tau)$ was further expanded in powers of the invariants ρ and τ. All perturbative results were recovered this way, that is, the one-loop results obtained either in $d = 4-\epsilon$ or in $d = 2+\epsilon$. Note that around $d=2$, it is necessary to take into account the so-called "current-term" – $(\vec{\phi}_1\cdot\partial\vec{\phi}_2 - \vec{\phi}_2\cdot\partial\vec{\phi}_1)^2$ – to get the phenomenon of enlarged symmetry at the fixed point [56], although it is irrelevant by power-counting in the vicinity of $d=4$. In $d=3$, the dimension in which we are interested in this article, such a term should not contribute significantly. We however keep it as we are tracking possible weaknesses of previous NPRG approaches.

IV. RENORMALIZATION GROUP EQUATIONS

We now present the RG equations relevant to non-collinear magnets. In the case of a model with $O(N)\times O(2)$ symmetry the exact flow equation Eq.(9) writes:

$$\partial_t\Gamma_k[\vec{\phi}_1,\vec{\phi}_2] = \frac{1}{2}\mathrm{Tr}\int_q \dot{R}_k(q)\left(\Gamma_k^{(2)}[q,-q,\vec{\phi}_1,\vec{\phi}_2] + R_k\right)^{-1} \tag{21}$$

where $\Gamma_k^{(2)}[q,-q,\vec{\phi}_1,\vec{\phi}_2]$ is the Fourier transform of the second functional derivatives of Γ_k:

$$\Gamma^{(2)}_{k,(a,i),(b,j)}[x,y,\vec{\phi}_1,\vec{\phi}_2] = \frac{\delta\Gamma_k[\vec{\phi}_1,\vec{\phi}_2]}{\delta\phi_a^i(x)\delta\phi_b^j(y)} \tag{22}$$

where $a,b=1,2$ and $i,j=1,\cdots,N$.

The flow equation for the effective potential $U_k(\rho,\tau)$ follows from its definition:

$$U_k(\rho,\tau) = \frac{1}{\Omega}\Gamma_k[\vec{\phi}_1,\vec{\phi}_2]\Big|_\Phi \tag{23}$$

where Ω is the volume of the system and Φ a constant field configuration. Since U_k is an O(N)×O(2) invariant, it is possible to use O(N)×O(2) transformations to simplify as much as possible the configuration Φ in which its RG flow (21) is evaluated. It is easy to show using these transformations that one can to recast any constant matrix Φ in a diagonal "form":

$$\Phi = U\Phi_D V \quad \text{with} \quad U \in O(N) \quad \text{and} \quad V \in O(2) \tag{24}$$

with:

$$\Phi_D = \begin{pmatrix} \phi_1 & 0 \\ 0 & \phi_2 \\ 0 & 0 \\ \vdots & \vdots \\ 0 & 0 \end{pmatrix} \tag{25}$$

where ϕ_1 and ϕ_2 are constants.

The – derivative – coefficients Z_k and ω_k are defined by:

$$Z_k = \frac{(2\pi)^d}{\delta(0)} \lim_{p^2\to 0} \frac{d}{dp^2} \left(\frac{\partial^2 \Gamma_k}{\delta\phi_1^1(p)\delta\phi_1^1(-p)}\bigg|_{\Phi_I} \right) \tag{26}$$

$$\frac{\omega_k}{2} = \frac{(2\pi)^d}{\kappa\delta(0)} \lim_{p^2\to 0} \frac{d}{dp^2} \left(\frac{\partial^2 \Gamma_k}{\delta\phi_1^2(p)\delta\phi_1^2(-p)}\bigg|_{\Phi_I} \right) - \frac{Z_k}{\kappa}, \tag{27}$$

where we choose a uniform field configuration Φ_I proportional to the identity:

$$\Phi_I = \begin{pmatrix} \sqrt{\kappa} & 0 \\ 0 & \sqrt{\kappa} \\ 0 & 0 \\ \vdots & \vdots \\ 0 & 0 \end{pmatrix} \tag{28}$$

$\sqrt{\kappa}$ being a constant that can be different from the minimum ϕ of the potential, Eq.(16). Finally the running anomalous dimension η_k is defined by $\eta_k = -\partial_t \log Z_k$.

The flow equation for the potential writes in terms of the various propagators associated with the mass spectrum of the model (see Appendix (A)):

$$\begin{aligned} \partial_t U_k(\rho,\tau) \;=\; & \frac{1}{2}\int_q \dot{R}_k(q^2) \Bigg[\frac{1}{Z_k q^2 + R_k(q^2) + m_{1+}^2} + \frac{1}{Z_k q^2 + R_k(q^2) + m_{1-}^2} \\ & + \frac{1}{Z_k q^2 + R_k(q^2) + m_{2+}^2} + \frac{1}{Z_k q^2 + R_k(q^2) + m_{2-}^2} \\ & + (N-2)\left(\frac{1}{Z_k q^2 + R_k(q^2) + m_{3+}^2} + \frac{1}{Z_k q^2 + R_k(q^2) + m_{3-}^2} \right) \Bigg] \end{aligned} \tag{29}$$

where the (momentum-dependent) square "masses" are given by:

$$\begin{cases} m_{1\pm}^2 \;= 2U_k^{(1,0)} + 2\rho U_k^{(2,0)} + \rho U_k^{(0,1)} + 2\rho\tau U_k^{(0,2)} + 8\tau U_k^{(1,1)} \\ \qquad\quad \pm \left\{ \tau \left(4U_k^{(0,1)} + 4U_k^{(2,0)} + 4\tau U_k^{(0,2)} + 4\rho U_k^{(1,1)} \right)^2 + \left(\rho^2 - 4\tau\right) \left(2U_k^{(2,0)} - U_k^{(0,1)} - 2\tau U_k^{(0,2)} \right)^2 \right\}^{\frac{1}{2}} \\ m_{2\pm}^2 \;= 2U_k^{(1,0)} + \rho U_k^{(0,1)} + \frac{\omega_k}{4}\rho\, q^2 \pm \frac{1}{2}\left\{ \omega_k^2 \tau q^4 + \left(\rho^2 - 4\tau\right) \left(-\frac{\omega_k}{2} q^2 + 2U_k^{(0,1)} \right)^2 \right\}^{\frac{1}{2}} \\ m_{3\pm}^2 \;= 2U_k^{(1,0)} \pm 2\sqrt{\tau} U_k^{(0,1)} \end{cases} \tag{30}$$

with $U_k^{(m,n)} = \partial^{m+n} U_k(\rho,\tau)/\partial^m\rho\,\partial^n\tau$, $\rho = {\phi_1}^2 + {\phi_2}^2$ and $\tau = ({\phi_1}^2 - {\phi_2}^2)^2$ where ϕ_1 and ϕ_2 parametrize the configuration Eq.(25).

We are interested, in the following, in fixed points of the RG flow equations. Finding them requires to work with dimensionless renormalized quantities that are defined by: $\tilde{\rho} = Z_k k^{2-d}\rho$, $\tilde{\tau} = Z_k^2 k^{2(2-d)}\tau$, $\widetilde{U}_k(\tilde{\rho},\tilde{\tau}) = k^{-d}U_k(\rho,\tau)$, $\widetilde{\omega}_k = Z_k^{-2}k^{d-2}\omega_k$, $y = q^2/k^2$, $r(y) = R_k(yk^2)/Z_k y k^2$. In terms of these variables the flow equation of the potential writes:

$$\begin{aligned} \partial_t \widetilde{U}_k \;= & -d\widetilde{U}_k(\tilde{\rho},\tilde{\tau}) + (d-2+\eta_k)\Big[\tilde{\rho}\widetilde{U}_k^{(1,0)}(\tilde{\rho},\tilde{\tau}) \\ & + 2\tilde{\tau}\widetilde{U}_k^{(0,1)}(\tilde{\rho},\tilde{\tau})\Big] + 2v_d \Big[l_0^d(\widetilde{m}_{1+}^2) + l_0^d(\widetilde{m}_{1-}^2) \\ & + l_0^d(\widetilde{m}_{2+}^2) + l_0^d(\widetilde{m}_{2-}^2) + (N-2)\big(l_0^d(\widetilde{m}_{3+}^2) + l_0^d(\widetilde{m}_{3-}^2)\big)\Big] \end{aligned} \tag{31}$$

where $v_d^{-1} = 2^{d+1}\pi^{d/2}\Gamma[d/2]$, $\widetilde{m}_i$ are the dimensionless analogues of the masses defined in Eqs.(30) and the threshold functions $l_n^d(w)$ are defined by:

$$l_n^d(w) = -\frac{n+\delta_{n,0}}{2}\int_0^\infty dy\; y^{d/2}\frac{\eta_k r(y) + 2yr'(y)}{[y(1+r(y))+w]^{n+1}}. \tag{32}$$

The RG equations for the running anomalous dimension η_k and the coupling constant ω_k are given in terms of dimensionless quantities by:

$$\begin{aligned}\eta_k \;=\; & \frac{2v_d}{d}\Big[d\tilde{\omega}_k\, l_{1,0}^d\left(\widetilde{m}_3^{\,2},0,0\right) + 64\tilde{\kappa}\,(\widetilde{U}_k^{(0,1)})^2 m_{2,2}^d\left(\widetilde{m}_3^{\,2},\widetilde{m}_{1-}^{\,2},0\right) + 128\tilde{\kappa}\,(\widetilde{U}_k^{(2,0)})^2 m_{2,2}^d\left(\widetilde{m}_3^{\,2},\widetilde{m}_{1+}^{\,2},0\right)\\ & +(d-2)\tilde{\kappa}\tilde{\omega}_k^2 l_{1,1}^{d+2}\left(\widetilde{m}_3^{\,2},\widetilde{m}_3^{\,2},\tilde{\kappa}\tilde{\omega}_k\right) + 2\tilde{\kappa}\tilde{\omega}_k^2 m_{2,2}^{d+4}\left(\widetilde{m}_3^{\,2},\widetilde{m}_3^{\,2},\tilde{\kappa}\tilde{\omega}_k\right) - 2\tilde{\kappa}\tilde{\omega}_k^2 n_{1,2}^{d+2}\left(\widetilde{m}_3^{\,2},\widetilde{m}_3^{\,2},\tilde{\kappa}\tilde{\omega}_k\right)\\ & +2\tilde{\kappa}\tilde{\omega}_k^2 n_{2,1}^{d+2}\left(\widetilde{m}_3^{\,2},\widetilde{m}_3^{\,2},\tilde{\kappa}\tilde{\omega}_k\right) - 2\tilde{\kappa}^2\tilde{\omega}_k^3 l_{1,2}^{d+4}\left(\widetilde{m}_3^{\,2},\widetilde{m}_3^{\,2},\tilde{\kappa}\tilde{\omega}_k\right) + 2\tilde{\kappa}^2\tilde{\omega}_k^3 n_{2,2}^{d+4}\left(\widetilde{m}_3^{\,2},\widetilde{m}_3^{\,2},\tilde{\kappa}\tilde{\omega}_k\right)\Big]\end{aligned} \tag{33}$$

$$\begin{aligned}\frac{d\tilde{\omega}_k}{dt} \;=\; & (d-2+2\eta)\,\tilde{\omega}_k + \frac{2v_d}{d}\Bigg[\frac{d\tilde{\omega}_k}{\tilde{\kappa}}\big(l_{1,0}^d(\widetilde{m}_3^{\,2},0,0) - l_{1,0}^d(\widetilde{m}_{1+}^{\,2},0,0)\big) + (d-2)\tilde{\omega}_k^2\, l_{1,1}^{d+2}(\widetilde{m}_3^{\,2},\widetilde{m}_3^{\,2},\tilde{\kappa}\tilde{\omega}_k)\\ & +\;(10-d)\,\tilde{\omega}_k^2\, l_{1,1}^{d+2}(\widetilde{m}_{1+}^{\,2},\widetilde{m}_3^{\,2},\tilde{\kappa}\tilde{\omega}_k) - 2\tilde{\kappa}\tilde{\omega}_k^3\, l_{1,2}^{d+4}(\widetilde{m}_3^{\,2},\widetilde{m}_3^{\,2},\tilde{\kappa}\tilde{\omega}_k) + 6\tilde{\kappa}\tilde{\omega}_k^3\, l_{1,2}^{d+4}(\widetilde{m}_{1+}^{\,2},\widetilde{m}_3^{\,2},\tilde{\kappa}\tilde{\omega}_k)\\ & +\;4(N-2)\,\tilde{\omega}_k^2\, l_{2,0}^{d+2}(\widetilde{m}_3^{\,2},0,0) + 4\tilde{\omega}_k^2\, l_{2,0}^{d+2}(\widetilde{m}_{1-}^{\,2},0,0) + 64(\widetilde{U}_k^{(0,1)})^2 m_{2,2}^d\left(\widetilde{m}_3^{\,2},\widetilde{m}_{1-}^{\,2},0\right) + 2\tilde{\omega}_k^2 m_{2,2}^{d+4}\left(\widetilde{m}_3^{\,2},\widetilde{m}_3^{\,2},\tilde{\kappa}\tilde{\omega}_k\right)\\ & -\;2\tilde{\omega}_k^2 m_{2,2}^{d+4}\left(\widetilde{m}_{1+}^{\,2},\widetilde{m}_3^{\,2},\tilde{\kappa}\tilde{\omega}_k\right) - 2\tilde{\omega}_k^2 n_{1,2}^{d+2}\left(\widetilde{m}_3^{\,2},\widetilde{m}_3^{\,2},\tilde{\kappa}\tilde{\omega}_k\right) + 6\tilde{\omega}_k^2 n_{1,2}^{d+2}\left(\widetilde{m}_{1+}^{\,2},\widetilde{m}_3^{\,2},\tilde{\kappa}\tilde{\omega}_k\right) + 2\tilde{\omega}_k^2 n_{2,1}^{d+2}\left(\widetilde{m}_3^{\,2},\widetilde{m}_3^{\,2},\tilde{\kappa}\tilde{\omega}_k\right)\\ & -\;6\tilde{\omega}_k^2 n_{2,1}^{d+2}\left(\widetilde{m}_{1+}^{\,2},\widetilde{m}_3^{\,2},\tilde{\kappa}\tilde{\omega}_k\right) + 128(\widetilde{U}_k^{(2,0)})^2\left(m_{2,2}^d\left(\widetilde{m}_3^{\,2},\widetilde{m}_{1+}^{\,2},0\right) - m_{2,2}^d\left(\widetilde{m}_{1+}^{\,2},\widetilde{m}_3^{\,2},0\right) - \tilde{\kappa}\tilde{\omega}_k n_{2,2}^d\left(\widetilde{m}_{1+}^{\,2},\widetilde{m}_3^{\,2},\tilde{\kappa}\tilde{\omega}_k\right)\right)\\ & +\;8\widetilde{U}_k^{(2,0)}\Big(d\, l_{1,1}^d(\widetilde{m}_{1+}^{\,2},\widetilde{m}_3^{\,2},\tilde{\kappa}\tilde{\omega}_k) - 6\tilde{\kappa}\tilde{\omega}_k l_{1,2}^{d+2}(\widetilde{m}_{1+}^{\,2},\widetilde{m}_3^{\,2},\tilde{\kappa}\tilde{\omega}_k) + 4m_{2,2}^{d+2}\left(\widetilde{m}_{1+}^{\,2},\widetilde{m}_3^{\,2},\tilde{\kappa}\tilde{\omega}_k\right) - 6n_{1,2}^d\left(\widetilde{m}_{1+}^{\,2},\widetilde{m}_3^{\,2},\tilde{\kappa}\tilde{\omega}_k\right)\\ & +\;6n_{2,1}^{d+2}\left(\widetilde{m}_{1+}^{\,2},\widetilde{m}_3^{\,2},\tilde{\kappa}\tilde{\omega}_k\right) + 4\tilde{\kappa}\tilde{\omega}_k n_{2,2}^{d+2}\left(\widetilde{m}_{1+}^{\,2},\widetilde{m}_3^{\,2},\tilde{\kappa}\tilde{\omega}_k\right)\Big) + 2\tilde{\kappa}\tilde{\omega}_k^3 n_{2,2}^{d+4}\left(\widetilde{m}_3^{\,2},\widetilde{m}_3^{\,2},\tilde{\kappa}\tilde{\omega}_k\right) - 2\tilde{\kappa}\tilde{\omega}_k^3 n_{2,2}^{d+4}\left(\widetilde{m}_{1+}^{\,2},\widetilde{m}_3^{\,2},\tilde{\kappa}\tilde{\omega}_k\right)\Bigg]\end{aligned} \tag{34}$$

where the masses are evaluated in the configuration Φ_I, Eq.(28) – where $\tau = 0$ – and are given by:

$$\begin{cases} \widetilde{m}_{1+}^{\,2} = 2\widetilde{U}_k^{(1,0)} + 8\tilde{\kappa}\widetilde{U}_k^{(2,0)} \\ \widetilde{m}_{1-}^{\,2} = \widetilde{m}_{2+}^{\,2} = 2\widetilde{U}_k^{(1,0)} + 4\tilde{\kappa}\widetilde{U}_k^{(0,1)} \\ \widetilde{m}_3^{\,2} = \widetilde{m}_{3+}^{\,2} = \widetilde{m}_{3-}^{\,2} = \widetilde{m}_{2-}^{\,2} = 2\widetilde{U}_k^{(1,0)} \end{cases} \tag{35}$$

where $U_k^{(a,b)}$ stands here for $U_k^{(a,b)}(\tilde{\rho} = 2\tilde{\kappa}, \tau = 0)$ and where the threshold functions l_{n_1,n_2}^d, m_{n_1,n_2}^d and n_{n_1,n_2}^d are given in the Appendix (B).

V. FIELD-SEMI-EXPANSION

The part of the potential that *a priori* needs to be represented as accurately as possible is the vicinity of the minimum Eq.(16) since it describes the thermodynamics of the system. The minimum occurs at a finite value ρ and at vanishing τ. We thus expect that the non trivial field dependence occurs in the ρ-direction and not in the τ one. The idea of the field-semi-expansion is thus to keep the full ρ-dependence of U_k and to expand it in powers of τ:

$$\widetilde{U}_k(\tilde{\rho},\tilde{\tau}) = \sum_{p=0}^{p_{\max}} \widetilde{U}_{p,k}(\tilde{\rho})\;\tilde{\tau}^p\;. \tag{36}$$

The flow of the functions $\widetilde{U}_{p,k}(\tilde{\rho})$ can be easily obtained by differentiating Eq.(31) with respect to τ. We have truncated the expansion at $p_{\max} = 2, 3$ and 4. For the sake of simplicity we only display the flow of $\widetilde{U}_{0,k}(\tilde{\rho})$:

$$\begin{aligned}\partial_t \widetilde{U}_{0,k}(\tilde{\rho}) \;=\; & -d\,\widetilde{U}_{0,k}(\tilde{\rho}) + (d-2+\eta_k)\,\tilde{\rho}\,\widetilde{U}'_{0,k}(\tilde{\rho})\\ & +2\,v_d\left[l_{1,0}^d(\widetilde{m}_{1+}^{\,2},0,0) + 2\,l_{1,0}^d(\widetilde{m}_{1-}^{\,2},0,0)\right.\\ & \left.+l_{1,0}^d(0,\widetilde{m}_{1-}^{\,2},\tilde{\rho}\tilde{\omega}_k/2) + 2(N-2)\;l_{1,0}^d(\widetilde{m}_{3+}^{\,2},0,0)\right]\end{aligned} \tag{37}$$

with: $\widetilde{U}'_{0,k}(\tilde{\rho}) = d\widetilde{U}_{0,k}(\tilde{\rho})/d\tilde{\rho}$ and where the square masses are given by:

$$\begin{cases} \widetilde{m}^2_{1+} = 2\widetilde{U}'_{0,k}(\tilde{\rho}) + 4\tilde{\rho}\widetilde{U}''_{0,k}(\tilde{\rho}) \\ \widetilde{m}^2_{1-} = 2\widetilde{U}'_{0,k}(\tilde{\rho}) + 2\tilde{\rho}\widetilde{U}_{1,k}(\tilde{\rho}) \\ \widetilde{m}^2_{3+} = 2\widetilde{U}'_{0,k}(\tilde{\rho}) \ . \end{cases} \tag{38}$$

A. Procedure

In order to integrate the RG flow equations of the functions $\widetilde{U}_{p,k}(\tilde{\rho})$, we need an initial condition, that is, their values at $k = \Lambda$. We choose the usual Ginzburg-Landau-Wilson potential:

$$\widetilde{U}_{k=\Lambda}(\rho, \tau) = \widetilde{r}_\Lambda\, \widetilde{\rho} + \widetilde{g}_{1,\Lambda}\, \widetilde{\rho}^2 + \widetilde{g}_{2,\Lambda}\, \widetilde{\tau} \tag{39}$$

which implies that $\widetilde{U}_{0,k=\Lambda}(\rho) = \widetilde{r}_\Lambda\, \widetilde{\rho} + \widetilde{g}_{1,\Lambda}\widetilde{\rho}^2$, $\widetilde{U}_{1,k=\Lambda}(\rho) = \widetilde{g}_{2,\Lambda}\widetilde{\tau}$ and $\widetilde{U}_{p>1,k=\Lambda}(\rho) = 0$. Criticality can be reached by varying the mass parameter $\widetilde{r}_\Lambda$ while keeping fixed $\widetilde{g}_{1,\Lambda}$ and $\widetilde{g}_{2,\Lambda}$.This can be repeated in principle in any dimension d and for all values of N greater than $N_c(d)$. We focus on the three dimensional case and thus on the value of $N_c(d = 3)$. We recall that $N_c(d)$ results from the collapse of two fixed points, one stable – the chiral C_+ – and one unstable – the anti-chiral C_- – when N is decreased from $N > N_c(d)$ to $N_c(d)$. These two fixed points are related by a RG flow line. When C_+ and C_- get closer, the speed of the flow decreases and vanishes at $N = N_c(d)$. Thus, a way to determine $N_c(d)$ consists in identifying the value of N for which the first correction to scaling critical exponent ω vanishes. In order to compute this quantity, we parametrize the potential close to the fixed point by:

$$\widetilde{U}_k(\widetilde{\rho}, \widetilde{\tau}) = \widetilde{U}^*(\widetilde{\rho}, \widetilde{\tau}) + \widetilde{F}(\widetilde{\rho}, \widetilde{\tau})\, e^{-t/\nu} + \widetilde{G}(\widetilde{\rho}, \widetilde{\tau})\, e^{\omega t} \tag{40}$$

where ν is the usual critical exponent associated with the relevant direction and ω the subleading critical exponent.

B. LPA

In order to measure the impact of the derivative terms η_k and ω_k on $N_c(d = 3)$ we perform two calculations, one where these two coupling constants are set to 0 (LPA) and the other one where we take them into account (LPA'). As for the potential we consider, in the expansion Eq.(36), the functions $\widetilde{U}_{p,k}(\tilde{\rho})$ up to $p_{\max} = 4$. This allows us to analyze the convergence of the expansion in powers of τ. Finally we have *optimized* our results. Indeed, as well known, finite truncations of the effective action in the field and/or derivatives of the field induce a residual dependence of the physical quantities on the regulator R_k. By definition, an optimal regulator is such that the dependence of the physical quantity under study upon this regulator is minimal: this is the Principle of Minimal Sensitivity (PMS). Applied to the O(N) models, this principle indeed leads to the best determination of the critical exponents in $d = 3$ in the sense that the results thus obtained are closest to the Monte Carlo values [55, 57]. To optimize our results, we have used the exponential cut-off Eq.(6) that we have extended to a whole family of cut-off functions parametrized by a real number α:

$$R^\alpha_k(q^2) = \alpha \frac{Z_k\, q^2}{e^{q^2/k^2} - 1} \ . \tag{41}$$

We have varied α in order to reach a point of minimal sensitivity, *i.e.* a point where the physical quantities – here mainly $N_c(d)$, now denoted $N_c(d, \alpha)$ – are as insensitive as possible to α. This obviously corresponds to an extremum of $N_c(d, \alpha)$ as a function of α.

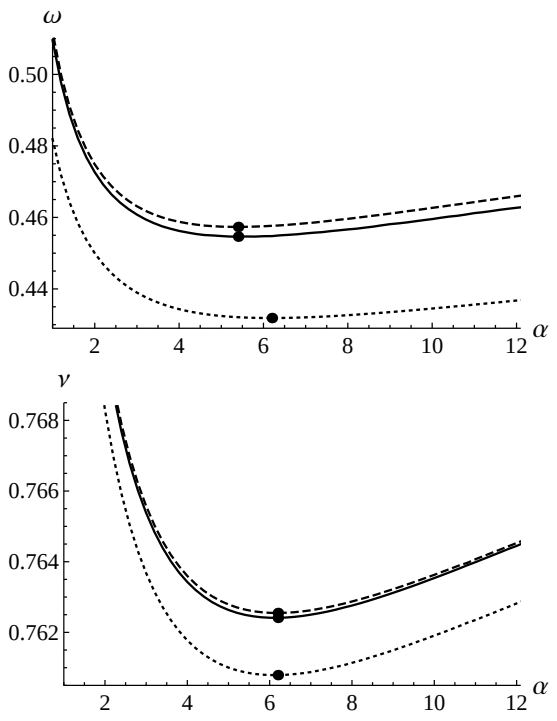

FIG. 1: $N = 6$, $d = 3$ case: critical exponents ω (top) and ν (bottom) as functions of the regulator parameter α (see Eq.(41)) calculated with $p_{\max} = 2$ (dotted curve), 3 (dashed curve) and 4 (solid curve). The black dots indicate the position of the minima of the curves.

1. *The N=6 case*

Before discussing the value of $N_c(d)$ within the derivative expansion, it is useful to consider a value of N where, very likely, there exists a fixed point C_+, *i.e.* $N > N_c(d = 3)$. We choose $N = 6$ since a clear second order phase transition has been found in this case by Monte Carlo simulations [58]. This allows us to check the

convergence of our computation. We find a stable fixed point for $N = 6$ in agreement with the results obtained numerically [58]. Figure (1) displays the correction-to-scaling critical exponent ω and the correlation length critical exponent ν as functions of the regulator parameter α with $p_{\max} = 2, 3$ and 4. First, one finds, for any $p_{\max}$, a unique extremum for each curve $\omega(d = 3, \alpha)$ and $\nu(d = 3, \alpha)$ when varying α. Second, one clearly observes a very good convergence with $p_{\max}$. This means that the PMS can be safely applied and that optimal values of the critical exponents can be determined. We find for $p_{\max} = 4$: $\omega_{\text{opt.}} = \omega(d = 3, \alpha = 5.4) = 0.455(5)$, $\nu_{\text{opt.}} = \nu(d = 3, \alpha = 6.2) = 0.7625(5)$ where error bars are evaluated from the difference between two successive orders of the field expansion. The value of ν can be compared with the Monte Carlo value $\nu = 0.700(11)$ [58]. Clearly our value of ν lies well above the numerical result. This relies on the fact that the effects of derivative terms have been neglected – see below.

2. $N_c(d = 3)$

We have then computed $N_c(d, \alpha)$ for $d = 3.8, 3.5, 3.0$ and 2.7 within the LPA and for $p_{\max} = 2, 3, 4$. In all cases, we find a maximum of $N_c(d, \alpha)$ when varying α, see Fig.(2). Moreover we find that $N_c(d, \alpha)$ at its maximum converges when $p_{\max}$ is increased. However, it appears that the speed of convergence decreases drastically with the dimension d, see Fig.(2). The convergence is very good for $3 < d < 4$ and becomes bad typically around $d = 2.8$. This is clearly a limit of the field expansion performed here. Indeed standard power counting implies the relevance of more and more powers of the field as the dimension is decreased. Another problem encountered at low dimensions is that there exists, for any dimension d lower that $d = 3$, a line $\widetilde{N}(d)$ located above the line $N_c(d)$ where the critical exponent ω vanishes; this is again an artifact of the field expansion. For these reasons we focus, in this article, on dimensions between $d = 2.8$ and $d = 4$. In the physically relevant $d = 3$ case one finds that the optimal value of $N_c(d = 3, \alpha)$ is given by $N_{c,\text{opt.}} = N_c(d = 3, \alpha = 6.2) = 4.68(2)$. This value is almost identical to that found by Zumbach [24–26] who has found $N_c(d = 3) = 4.7$ using the LPA implemented on the Polchinski equation *without* any field expansion. This suggests that our result for $N_c(d = 3)$ is almost converged as far the field expansion is concerned. This will be confirmed in section VI where we evaluate $N_c(d = 3)$ without any field expansion.

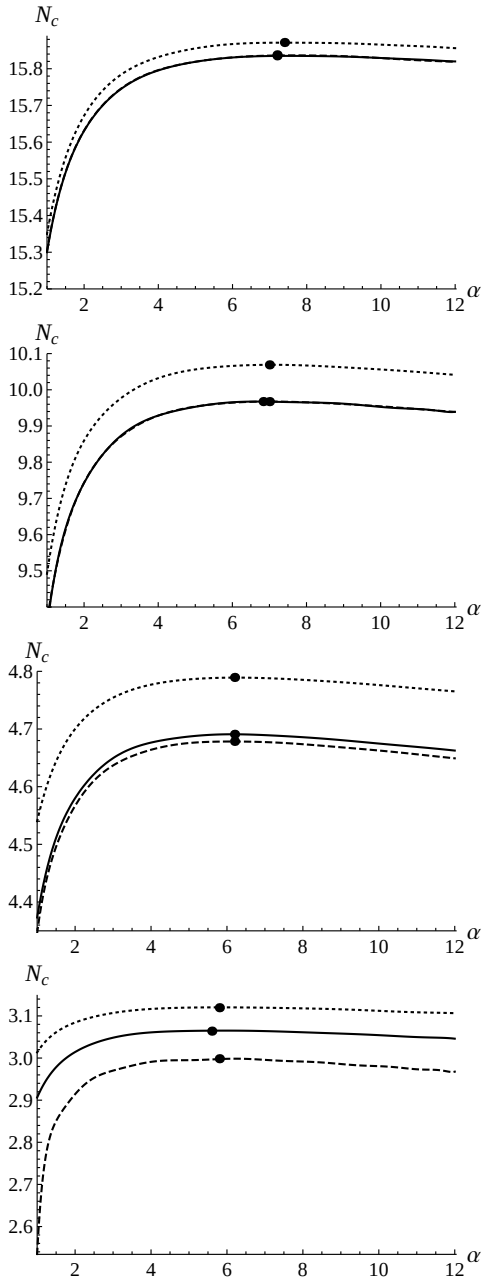

FIG. 2: $N_c(d, \alpha)$ obtained with the LPA with $p_{\max} = 2$ (dotted curve), $p_{\max} = 3$ (dashed curve) and $p_{\max} = 4$ (solid curve) for, from top to bottom: $d = 3.8$, $d = 3.5$, $d = 3$ and $d = 2.8$. For $d = 3.8$ and $d = 3.5$, the two curves obtained with $p_{\max} = 3$ and $p_{\max} = 4$ are superimposed at this scale. The black dots indicate the position of the minima of the curves.

C. LPA'

Let us now consider the contributions coming from the leading derivative terms and thus the impact of the anomalous dimension η_k and of the coupling constant ω_k onto $N_c(d)$. The corresponding flow equations are given by Eqs.(33) and (34). The flow of these new coupling constants involves a new degree of freedom which is the choice of the field configuration Φ_I where they are evaluated (see Eqs.(26), (27) and (28)). In order to implement the PMS we vary Φ_I and look for a extremum of the quantities we compute, that is, the critical exponents for $N = 7$, $N = 6$ and finally $N_c(d)$.

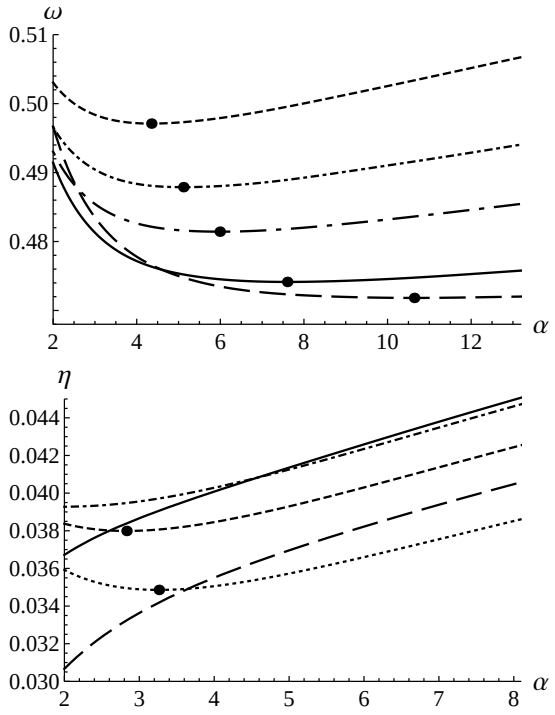

FIG. 3: Critical exponents ω (top) and η (bottom) as functions of the parameter α for $N = 7$, $d = 3$, $p_{\max} = 4$. Curves of different styles correspond to various values of $\rho_{\rm fix}$: the dotted curve corresponds to $\rho_{\rm fix}$ =0.4, the dashed curve to $\rho_{\rm fix}$ =0.5, the dotdashed curve to $\rho_{\rm fix}$ =0.6, the long dotdashed curve to $\rho_{\rm fix}$ =0.7, the solid curve to $\rho_{\rm fix}$ =0.9 and the long dashed curve to $\rho_{\rm fix}$=1.2. The black dots indicate the position of the minima of the curves.

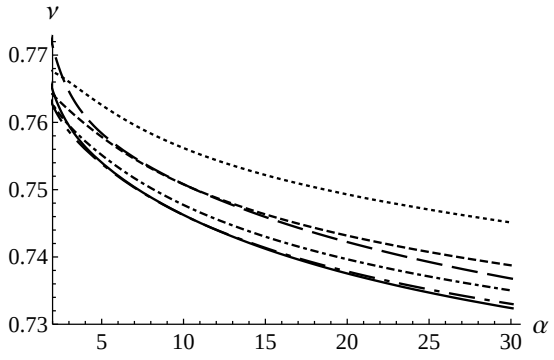

FIG. 4: Critical exponent ν as a function of the parameter α for $N = 7$, $d = 3$, $p_{\max} = 4$. The dotted curve corresponds to $\rho_{\rm fix}$ =0.4, the dashed curve to $\rho_{\rm fix}$ =0.5, the dotdashed curve to $\rho_{\rm fix}$ =0.6, the long dotdashed curve to $\rho_{\rm fix}$ =0.7, the solid curve to $\rho_{\rm fix}$ =0.9 and the long dashed curve to $\rho_{\rm fix}$=1.2. There are no extrema for the different curves.

1. *The N=7 case*

We first address the $N = 7$ case which corresponds to the smallest integer value of N for which there is a stable fixed point both within the NPRG and the perturbative approaches performed either within the ϵ- or pseudo-ϵ- expansion. We find a fixed point for all $p_{\max}$. The curves for the critical exponents ω, η and ν as functions of α computed with $p_{\max} = 4$ in $d = 3$ are given in Fig.(3) and Fig.(4). The different curves correspond to different values of Φ_I or, equivalently, to different values of $\rho_{\rm fix} \equiv 2\kappa$, going from 0.4 to 1.2. Although calculations were performed for all $\rho_{\rm fix}$ between 0.4 to 1.2 with step 0.1 we present only the main curves in order not to overload the figures. The results for ω show that a stationary curve is obtained for $\rho_{\rm fix} \simeq 0.9$ (solid curve in Fig.(3)). For the corresponding curve, the minimum is reached for $\alpha \simeq 7.5$ which provides the optimal value $\omega_{\rm opt.} = \omega(d = 3, \alpha = 7.5) \simeq 0.475$. For η, the stationary curve is obtained for $\rho_{\rm fix} \simeq 0.6$ (dotdashed curve in Fig.(3)). In this case however there is no genuine stationarity in α. By continuity with the results obtained for $\rho_{\rm fix} \simeq 0.4$ and $\rho_{\rm fix} \simeq 0.5$ (respectively dotted and dashed curves on Fig.(3)) for which we get genuine minima one can consider that there exists, in the case $\rho_{\rm fix} \simeq 0.6$, a quasi-minimum at $\alpha = 2$. This provides the almost optimal value $\eta_{\rm opt.} = \eta(d = 3, \alpha = 2) = 0.039$. The determination of ν is more problematic, see Fig.(4). Indeed, whereas there is a stationary curve when varying $\rho_{\rm fix}$ at $\rho_{\rm fix} = 0.7$ (long dotdashed curve in Fig.(4)) there is no extremum when varying α. However as the curve $\nu(d = 3, \alpha)$ varies only weakly with α for large values of α one can provide a rough estimate of $\nu(d = 3, \alpha)$ by the range $[0.730 - 0.740]$. We finally provide the values of the critical exponents with estimation of error bars: $\omega = 0.475(2)$, $\eta = 0.039(2)$ and $\nu = 0.735(5)$. These values can be compared with the those obtained perturbatively. The ϵ-expansion performed at five loops within the $\overline{MS}$ scheme [18] provides $\omega = 0.33(10)$, $\gamma = 1.39(6)$ and $\nu = 0.71(4)$ that leads to, through scaling relations, $\eta = 0.042(4)$. Computations, still at five-loop order and within the $\overline{MS}$ scheme *without* ϵ-expansion [12] leads to $\omega = 0.5(2)$, $\eta = 0.047(15)$ and $\nu = 0.68(4)$. Finally within a six-loop computation performed using the zero momentum massive scheme and resummed using the conformal mapping technique (Padé approximant techniques provide close results) one finds [23] : $\omega = 0.23(5)$, $\eta = 0.042(2)$ and $\nu = 0.68(2)$. Being given the large error bars provided by both the perturbative and non-perturbative computations the results are all compatible so that the $N = 7$ does not show strong indications of a disagreement between the different approaches.

2. *The N=6 case*

For $N = 6$, we again find a fixed point for all $p_{\max}$. The curves for the critical exponents ω, η and ν as functions of α computed with $p_{\max} = 4$ in $d = 3$ are given in Fig.(5) and Fig.(6). For ω a stationary curve is obtained for $\rho_{\rm fix} \simeq 0.9$ (solid curve in Fig.(5)) with a minimum reached for $\alpha \simeq 10.5$. This provides the optimal value

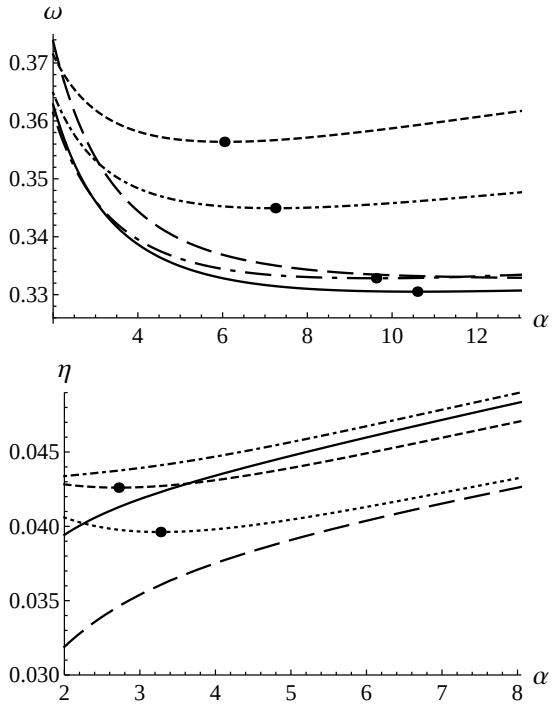

FIG. 5: Critical exponents ω (top) and η (bottom) as functions of the parameter α for $N = 6$, $d = 3$, $p_{\max} = 4$. Curves of different styles correspond to various values of $\rho_{\rm fix}$: the dotted curve corresponds to $\rho_{\rm fix}$ =0.4, the dashed curve to $\rho_{\rm fix}$ =0.5, the dotdashed curve to $\rho_{\rm fix}$ =0.6, the long dotdashed curve to $\rho_{\rm fix}$ =0.8, the solid curve to $\rho_{\rm fix}$ =0.9 and the long dashed curve to $\rho_{\rm fix}$=1.2.The black dots indicate the position of the minima of the curves.

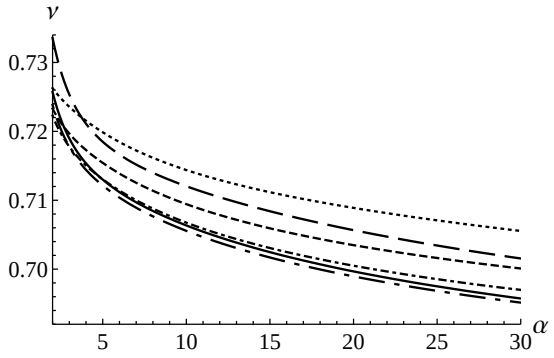

FIG. 6: Critical exponent ν as a function of the parameter α for $N = 6$, $d = 3$, $p_{\max} = 4$. The dotted curve corresponds to $\rho_{\rm fix}$ =0.4, the dashed curve to $\rho_{\rm fix}$ =0.5, the dotdashed curve to $\rho_{\rm fix}$ =0.6, the long dotdashed curve to $\rho_{\rm fix}$ =0.8, the solid curve to $\rho_{\rm fix}$ =0.9 and the long dashed curve to $\rho_{\rm fix}$=1.2. There are no extrema for the different curves.

$\omega_{\rm opt.} = \omega(d = 3, \alpha = 10.5) \simeq 0.330$. For η, a stationary curve is obtained for $\rho_{\rm fix} \simeq 0.6$ (dotted-dashed curve in Fig.(5)). In this case, again, there is no genuine stationarity in α. Note nevertheless that for close values of $\rho_{\rm fix}$ (of order 0.4–0.5, corresponding to dotted and dashed curves in Fig.(5)) one gets clear minima. By continuity this provides an almost optimal value of η lying between 0.040 and 0.045. The same problem as in the $N = 7$ case is encountered for ν – see Fig.(6) – since, whereas there is a stationary curve when varying $\rho_{\rm fix}$ at $\rho_{\rm fix} = 0.8$ (long dotdashed curve in Fig.(6)) there is no extremum when varying α. As in the $N = 7$ case one can consider the variation of $\nu(d = 3, \alpha)$ as smooth with α for large values of α and an estimate of $\nu(d = 3, \alpha)$ can be given by the range $[0.69 - 0.70]$. We finally provide the values of the critical exponents with estimation of error bars: $\omega = 0.330(5)$, $\eta = 0.042(2)$ and $\nu = 0.695(5)$. The critical exponent ν can be favorably compared with the Monte Carlo results $\nu = 0.700(11)$ [58], what provides indications of convergence of our computations. One can compare these results with those obtained using a five-loop computation and performed within the $\overline{MS}$ scheme *without* ϵ-expansion [12] for which a fixed point is found for all values of N. In the $N = 6$ case, these computations lead to $\eta = 0.052(14)$ and $\nu = 0.66(4)$. These values are compatible with both the NPRG and Monte Carlo results. However it is at the cost of large error bars, that are very likely consequences of the poor convergence of the computations performed at fixed dimensions already observed in [31–33].

3. $N_c(d = 3)$

Let us now consider $N_c(d = 3)$ computed with $p_{\max} = 4$ within the LPA'. We find an optimal value of $N_c(d = 3, \alpha)$ for $\rho_{\rm fix} \in [0.8, 0.9]$ (see solid and longdotdashed curves in Fig.(7)). However, there is no true extremum of $N_c(d = 3)$ in the direction of α for these values of $\rho_{\rm fix}$ although $N_c(d = 3)$ is almost insensitive to α for $\alpha \sim 15$, see Fig.(7). This provides the best possible value of $N_c(d = 3)$: $N_{c,\rm opt}(d = 3, \alpha = 15) = 5.24(2)$. The comparison with the value obtained using a usual field expansion [1, 27–30], $N_c(d = 3) = 5.1$, shows that the effects of high orders in the field neglected in previous approaches were not negligible. Moreover, compared with the value $N_c(d = 3) = 4.7$ obtained within the LPA, one sees that derivative terms also play an important role. Our value of $N_c(d = 3)$ can finally be compared with those obtained perturbatively via the ϵ- or pseudo-ϵ- expansions. Within the ϵ-expansion, one finds at five loops $N_c(d = 3) = 6.1(6)$ [18], and the pseudo-ϵ- expansion at six loops leads to $N_c(d = 3) = 6.22(12)$ [18] and $N_c(d = 3) = 6.23(21)$ [19]. The quantitative agreement is not excellent. One can suspect contributions of higher orders in derivatives of the field within the NPRG approach or/and contributions of higher orders in the loop expansions. However, from the qualitative point of view all these results agree as for the absence of a non trivial fixed point for $N = 2$ and $N = 3$.

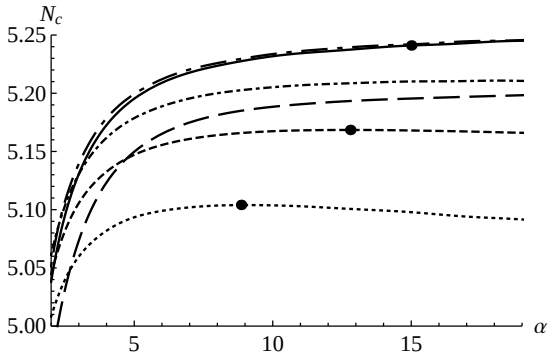

FIG. 7: $N_c(d = 3, \alpha)$ for $p_{\max} = 4$. The dotted curve corresponds to $\rho_{\rm fix}$ =0.4, the dashed curve to $\rho_{\rm fix}$ =0.5, the dotdashed curve to $\rho_{\rm fix}$ =0.6, the long dotdashed curve to $\rho_{\rm fix}$ =0.8, the solid curve to $\rho_{\rm fix}$ =0.9 and the long dashed curve to $\rho_{\rm fix}$=1.2. The black dots indicate the position of the minima of the curves.

D. The curve $N_c(d)$

Finally we have computed $N_c(d)$ for values of d going from $d = 2.8$ to $d = 4$. The corresponding (solid) curve is shown in Fig.(8) together with that (dashed) obtained within the perturbative five-loops ϵ-expansion of [23] and that (dotdashed) obtained within the perturbative six-loop *without* ϵ-expansion [12]. The qualitative agreement between the NPRG and the ϵ-expansion results is apparent although, quantitatively, there remain some relatively important gaps between the different values of $N_c(d)$ for some dimensions between $d = 3$ and $d = 4$. On the other hand, the singular character of the result obtained *without* ϵ-expansion – for which the curve $N_c(d)$ displays a S-like shape – is also obvious.

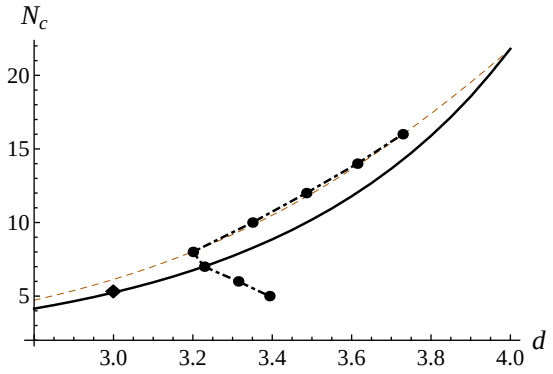

FIG. 8: Curves $N_c(d)$. Solid curve (this work): LPA' with four functions. Diamond (this work) $N_c(d = 3)$ obtained by LPA' with the full potential. Dashed curve : perturbative five loops ($\overline{MS}$ scheme) with ϵ-expansion [23]. Dotdashed curve with black points: perturbative six loops ($\overline{MS}$ scheme) without ϵ-expansion [12].

VI. FULL POTENTIAL APPROACH

We finally present preliminary results obtained when one takes into account the full field content of the effective potential. In this case we have employed the theta cut-off Eq.(7) what allows to obtain analytical expressions for the RG equations and thus a manageable integration of the RG flow. However due to the massive computational requirements of this approach we have focused our attention on the $d = 3$ case delaying the study of the general case in [59]. Note that, for simplicity, we set $\omega_k = 0$ which is justified by the observation that this coupling constant plays a minor role around $d = 3$. First we have determined the critical exponent in the $N = 7$ case and have obtained: $\eta = 0.0438$ and $\nu = 0.760$. These values are roughly compatible with those obtained within the field-semi-expansion ($\eta = 0.039(2)$ and $\nu = 0.735(5)$). This is also true in the $N = 6$ case for which one finds: $\eta = 0.0487$ and $\nu = 0.716$ to be compared to $\eta = 0.042(2)$ and $\nu = 0.695(5)$, with a critical exponent ν still compatible with that found within the Monte Carlo approach ($\nu = 0.700(11)$). As for $N_c(d = 3)$ the full potential approach leads to the value $N_c(d = 3) = 4.8$ using the LPA. Compared to the value $N_c(d = 3) = 4.7$ obtained within the LPA in a field-semi-expansion this shows that our expansion was almost converged, as claimed in section V B. Taking now into account the derivative terms at lowest order (LPA') one finds: $N_c(d = 3) = 5.4$, see Fig.(8). Compared with the value $N_c(d = 3) = 5.24(2)$ obtained within the LPA' in a field-semi-expansion this confirms that the field expansion is almost converged. But compared to the value $N_c(d = 3) = 4.8$ obtained using the LPA this also shows that the effects of derivatives terms are not negligible. Clearly one cannot firmly conclude that convergence of the derivative expansion has been reached and one can expect that higher order terms contribute. However it is very unlikely that these derivative terms drastically change the overall shape of the curve $N_c(d)$ obtained here.

VII. CONCLUSION

We have investigated the behaviour of non-collinear magnets using a functional RG approach, focusing on the critical value $N_c(d)$. First, from the methodological point of view, our approach, that combines computations based on a field-semi-expansion and computations performed without any field expansion, confirms the validity of former approach to investigate complex systems. Second, as for the physics of frustrated magnets, our computations clearly favours a value of $N_c(d = 3)$ significantly larger than 3 excluding the occurrence of a second order phase transition in the physical $N = 2$ and $N = 3$ cases. Our result confirms ϵ- (and pseudo-ϵ-) expansions as well as early NPRG approaches based on the Polchinski and Wetterich equations. It contradicts both those obtained using fixed dimension perturbative approaches as well as

those resulting from recent CB approach. Up to now there is no indication of failure or even weakness coming from either ϵ–expansion or NPRG approaches. On the opposite the conclusion of second order phase transition obtained within fixed dimension approaches have been shown to be extremely dubious. There is no such suspicion concerning the CB approach. However several points must be clarified in this context. First, it is crucial to understand the status of the assumptions made and, in particular, that of the existence of scale invariance, in order to avoid a self-fulfilling prophecy. Second, the method should give an account of the existence of the anti-chiral fixed point C_- and the "dynamics" of C_+ and C_- that generates the curve $N_c(d)$ when N is lowered.

Acknowledgments

This work was supported in part by the 7th FP, IRSES project No 269139 Dynamics and Cooperative phenomena in complex physical and biological environments. M.D. thanks the LPTMC for hospitality during preparation of this work.

Appendix A: Propagator

The propagator of the model is a matrix whose components are given by the (Fourier transform of the) second derivative of Γ_k with respect to the field (see Eq.(22)) evaluated in the configuration Eq.(25). It is given by:

$$\Gamma^{(2)}_{k,(a,i),(b,j)}[q_1,q_2]+R_k(q)=\begin{pmatrix}
\Gamma_{k,(1,1),(1,1)} & \Gamma_{k,(1,1),(1,2)} & \Gamma_{k,(1,1),(2,1)} & \Gamma_{k,(1,1),(2,2)} & & & & \\
\Gamma_{k,(1,2),(1,1)} & \Gamma_{k,(1,2),(1,2)} & \Gamma_{k,(1,2),(2,1)} & \Gamma_{k,(1,2),(2,2)} & & & & \\
\Gamma_{k,(2,1),(1,1)} & \Gamma_{k,(2,1),(1,2)} & \Gamma_{k,(2,1),(2,1)} & \Gamma_{k,(2,1),(2,2)} & & 0 & & \\
\Gamma_{k,(2,2),(1,1)} & \Gamma_{k,(2,2),(1,2)} & \Gamma_{k,(2,2),(2,1)} & \Gamma_{k,(2,2),(2,2)} & & & & \\
 & & & & \ddots & & & \\
 & & & & & \Gamma_{k,(1,i>2),(1,i>2)} & & \\
 & & & & & & \Gamma_{k,(2,i>2),(2,i>2)} & \\
 & 0 & & & & & \ddots &
\end{pmatrix}, \tag{A1}$$

or, taking account of the vanishing components and the symmetries, by:

$$\Gamma^{(2)}_{k,(a,i),(b,j)}[q_1,q_2]+R_k(q)=\begin{pmatrix}
A & 0 & 0 & C & & & & \\
0 & E & D & 0 & & & & \\
0 & D & F & 0 & & 0 & & \\
C & 0 & 0 & B & & & & \\
 & & & & \ddots & & & \\
 & & & & & H & & \\
 & & & & & & G & \\
 & & & & & & & H \\
 & 0 & & & & & G & \\
 & & & & & & & \ddots
\end{pmatrix}, \tag{A2}$$

where the matrix elements A, B, C, D, E, F, G and H, are given by:

$$
\begin{aligned}
A &= Z_k q^2 + R_k(q^2) + 2U_k^{(1,0)} + ({\phi_1}^2 - {\phi_2}^2)U_k^{(0,1)} + {\phi_1}^2\left(4U_k^{(2,0)} + 4({\phi_1}^2 - {\phi_2}^2)U_k^{(1,1)} + 2U_k^{(0,1)} + ({\phi_1}^2 - {\phi_2}^2)^2 U_k^{(0,2)}\right)\\
B &= Z_k q^2 + R_k(q^2) + 2U_k^{(1,0)} - ({\phi_1}^2 - {\phi_2}^2)U_k^{(0,1)} + {\phi_2}^2\left(4U_k^{(2,0)} - 4({\phi_1}^2 - {\phi_2}^2)U_k^{(1,1)} + 2U_k^{(0,1)} + ({\phi_1}^2 - {\phi_2}^2)^2 U_k^{(0,2)}\right)
\end{aligned}
\tag{A3}
$$

$$
\begin{aligned}
C &= \phi_1\phi_2\left(4U_k^{(2,0)} - 2U_k^{(0,1)} - ({\phi_1}^2 - {\phi_2}^2)^2 U_k^{(0,2)}\right)\\
D &= \phi_1\phi_2\left(-\frac{\omega_k}{2}q^2 + 2U_k^{(0,1)}\right)
\end{aligned}
\tag{A4}
$$

$$
\begin{aligned}
E &= Z_k q^2 + R_k(q^2) + \frac{\omega_k}{2}{\phi_1}^2 q^2 + 2U_k^{(1,0)} + \rho U_k^{(0,1)}\\
F &= Z_k q^2 + R_k(q^2) + \frac{\omega_k}{2}{\phi_2}^2 q^2 + 2U_k^{(1,0)} + \rho U_k^{(0,1)}
\end{aligned}
\tag{A5}
$$

$$
\begin{aligned}
G &= Z_k q^2 + R_k(q^2) + 2U_k^{(1,0)} - ({\phi_1}^2 - {\phi_2}^2)U_k^{(0,1)}\\
H &= Z_k q^2 + R_k(q^2) + 2U_k^{(1,0)} + ({\phi_1}^2 - {\phi_2}^2)U_k^{(0,1)}
\end{aligned}
\tag{A6}
$$

The eigenvalues of Eq.(A2) are given by:

$$
\begin{aligned}
\lambda_{1,2} &= \frac{A+B\pm\sqrt{(A-B)^2+4C^2}}{2}\\
\lambda_{3,4} &= \frac{E+F\pm\sqrt{(E-F)^2+4D^2}}{2}
\end{aligned}
\tag{A7}
$$

$$
\lambda_5 = \cdots = \lambda_{2N-1} = H \qquad \lambda_6 = \cdots = \lambda_{2N} = G \tag{A8}
$$

Taking into account of the fact that in the configuration Eq.(25) that we consider to establish the equation of the effective potential one has: ${\phi_1}^2 + {\phi_2}^2 = \rho$ and $({\phi_1}^2 - {\phi_2}^2)^2 = 2\tau$ the eigenvalues read:

$$
\begin{aligned}
\lambda_{1\pm} &= Z_k q^2 + R_k(q^2) + 2U_k^{(1,0)} + 2\rho U_k^{(2,0)} + \rho U_k^{(0,1)} + \rho\tau U_k^{(0,2)} + 8\tau U_k^{(1,1)}\\
&\pm\left\{\tau\left(4U_k^{(0,1)} + 4U_k^{(2,0)} + 4\tau U_k^{(0,2)} + 4\rho U_k^{(1,1)}\right)^2 + \left(\rho^2 - 4\tau\right)\left(2U_k^{(2,0)} - U_k^{(0,1)} - 2\tau U_k^{(0,2)}\right)^2\right\}^{\frac{1}{2}}\\
&= Z_k q^2 + R_k(q^2) + m_{1\pm}^2
\end{aligned}
\tag{A9}
$$

$$
\begin{aligned}
\lambda_{2\pm} &= Z_k q^2 + R_k(q^2) + 2U_k^{(1,0)} + \rho U_k^{(0,1)} + \frac{\omega_k}{4}\rho\, q^2 \pm \frac{1}{2}\left\{\omega_k^2\tau q^4 + \left(\rho^2 - 4\tau\right)\left(-\frac{\omega_k}{2}q^2 + 2U_k^{(0,1)}\right)^2\right\}^{\frac{1}{2}}\\
&= Z_k q^2 + R_k(q^2) + m_{2\pm}^2
\end{aligned}
$$

where one has to take care about the fact that the "masses" m_{2+} and m_{2-} are momentum-dependent. There are moreover $N-2$ modes with eigenvalues λ_{3+} and $N-2$ modes with eigenvalues λ_{3-} with:

$$
\begin{aligned}
\lambda_{3\pm} &= Z_k q^2 + R_k(q^2) + 2U_k^{(1,0)} \pm 2\sqrt{\tau}U_k^{(0,1)}\\
&= Z_k q^2 + R_k(q^2) + m_{3\pm}^2\ .
\end{aligned}
\tag{A10}
$$

For completeness the mass spectrum at the minimum of the potential is given. In this case one has: $U_k^{(1,0)} = 0$ and $\tau = 0$. This implies that: $m_{1+}^2 = 4\rho U_k^{(2,0)}$, $m_{1-}^2 = 2\rho U_k^{(0,1)}$, $m_{2+}^2 = 2\rho U_k^{(0,1)} = m_{1-}^2$ and $m_{2-} = m_{3+} = m_{3-} = 0$. As a consequence one obtains the following spectrum: one massive singlet with square mass $m_s^2 = 4\rho U_k^{(2,0)}$, one massive doublet with square mass $m_d = 2\rho U_k^{(0,1)}$ and $2N-3$ Goldstone modes.

Appendix B: The threshold functions

We finally discuss the different threshold functions l, m and n appearing in the flow equations.

1. Definitions

The threshold functions are defined as:

$$\begin{aligned} l^d_{n_1,n_2}(w_1,w_2,w) &= -\frac{1}{2}\int_0^\infty dy \quad y^{d/2-1}\tilde{\partial}_t\left\{\frac{1}{(P_1+w_1)^{n_1}(P_2+w_2)^{n_2}}\right\} \\ m^d_{n_1,n_2}(w_1,w_2,w) &= -\frac{1}{2}\int_0^\infty dy \quad y^{d/2-1}\tilde{\partial}_t\left\{\frac{y(\partial_y P_1)^2}{(P_1+w_1)^{n_1}(P_2+w_2)^{n_2}}\right\} \\ n^d_{n_1,n_2}(w_1,w_2,w) &= -\frac{1}{2}\int_0^\infty dy \quad y^{d/2-1}\tilde{\partial}_t\left\{\frac{y\partial_y P_1}{(P_1+w_1)^{n_1}(P_2+w_2)^{n_2}}\right\} \end{aligned} \tag{B1}$$

where:

$$\begin{cases} P_1 = P_1(y) = y(1+r(y)) \\ P_2 = P_2(y,w) = y(1+r(y)+w) \end{cases} \tag{B2}$$

and $r(y)$ is the dimensionless cut-off: $r(y) = R_k(yk^2)/Z_k yk^2$.

We recall that the tilde in $\tilde{\partial}_t$ means that only the t dependence of the function R_k is to be considered. As a consequence, we should not consider the t-dependence of the coupling constants to perform this derivative. Therefore, in the preceding equations:

$$\tilde{\partial}_t P_i = \frac{\partial R_k}{\partial t}\frac{\partial P_i}{\partial R_k} = -y(\eta r(y) + 2yr'(y)). \tag{B3}$$

Now, threshold functions can be expressed as explicit integrals if we compute the action of $\tilde{\partial}_t$. To this end, it is interesting to notice the equality: $\tilde{\partial}_t\partial_y P_i = \partial_y\tilde{\partial}_t P_i$, so that:

$$\tilde{\partial}_t\partial_y r(y) = -\eta\Big(r(y)+yr'(y)\Big) - 2y\Big(2r'(y)+yr''(y)\Big) \tag{B4}$$

We then get:

$$l^d_{n_1,n_2}(w_1,w_2,w) = -\frac{1}{2}\int_0^\infty dy\; y^{d/2}\,\frac{\eta r(y)+2yr'(y)}{(P_1+w_1)^{n_1}(P_2+w_2)^{n_2}}\left(\frac{n_1}{P_1+w_1}+\frac{n_2}{P_2+w_2}\right) \tag{B5}$$

$$\begin{aligned} n^d_{n_1,n_2}(w_1,w_2,w) = -\frac{1}{2}\int_0^\infty dy\; y^{d/2}\frac{1}{(P_1+w_1)^{n_1}(P_2+w_2)^{n_2}}\Bigg\{ & y\Big(1+r(y)+yr'(y)\Big)\Big(\eta r(y)+2yr'(y)\Big)\times \\ & \left(\frac{n_1}{P_1+w_1}+\frac{n_2}{P_2+w_2}\right) - \eta\Big(r(y)+yr'(y)\Big) - 2y\Big(2r'(y)+yr''(y)\Big)\Bigg\} \end{aligned} \tag{B6}$$

$$\begin{aligned} m^d_{n_1,n_2}(w_1,w_2,w) = -\frac{1}{2}\int_0^\infty dy\; y^{d/2}\frac{1+r(y)+yr'(y)}{(P_1+w_1)^{n_1}(P_2+w_2)^{n_2}}\Bigg\{ & y\Big(1+r(y)+yr'(y)\Big)\Big(\eta r(y)+2yr'(y)\Big)\times \\ & \left(\frac{n_1}{P_1+w_1}+\frac{n_2}{P_2+w_2}\right) - 2\eta\Big(r(y)+yr'(y)\Big) - 4y\Big(2r'(y)+yr''(y)\Big)\Bigg\}. \end{aligned} \tag{B7}$$

[1] B. Delamotte, D. Mouhanna, and M. Tissier, Phys. Rev. B **69**, 134413 (2004).

[2] H. Kawamura, Phys. Rev. B **38**, 4916 (1988).

[3] H. Diep, Phys. Rev. B **39**, 397 (1989).
[4] D. Loison and K. D. Schotte, Eur. Phys. J. B **5**, 735 (1998).
[5] D. Loison and K. D. Schotte, Eur. Phys. J. B **14**, 125 (2000).
[6] M. Itakura, J. Phys. Soc. Jap. **72**, 74 (2003).
[7] A. Peles, B. W. Southern, B. Delamotte, D. Mouhanna, and M. Tissier, Phys. Rev. B **69**, 220408(R) (2004).
[8] S. Bekhechi, B. Southern, A. Peles, and D. Mouhanna, Phys. Rev. E **74**, 016109 (2006).
[9] G. Quirion, X. Han, M. L. Plumer, and M. Poirier, Phys. Rev. Lett. **97**, 077202 (2006).
[10] M. Zelli, K. Boese, and B. W. Southern, Phys. Rev. B **76**, 224407 (2007).
[11] V. T. Ngo and H. T. Diep, Phys. Rev. E **78**, 031119 (2008).
[12] P. Calabrese, P. Parruccini, A. Pelissetto, and E. Vicari, Phys. Rev. B **70**, 174439 (2004).
[13] D. R. T. Jones, A. Love, and M. A. Moore, J. Phys. C **9**, 743 (1976).
[14] D. Bailin, A. Love, and M. A. Moore, J. Phys. C **10**, 1159 (1977).
[15] T. Garel and P. Pfeuty, J. Phys. C **9**, L245 (1976).
[16] Z. Barak and M. B. Walker, Phys. Rev. B **25**, 1969 (1982).
[17] S. A. Antonenko, A. I. Sokolov, and K. B. Varnashev, Phys. Lett. A **208**, 161 (1995).
[18] P. Calabrese and P. Parruccini, Nucl. Phys. B **679**, 568 (2004).
[19] Yu. Holovatch, D. Ivaneyko, and B. Delamotte, J. Phys. A **37**, 3569 (2004).
[20] S. A. Antonenko and A. I. Sokolov, Phys. Rev. B **49**, 15901 (1994).
[21] A. Pelissetto, P. Rossi, and E. Vicari, Phys. Rev. B **63**, 140414(R) (2001).
[22] P. Calabrese, P. Parruccini, and A. I. Sokolov, Phys. Rev. B **66**, 180403(R) (2002).
[23] P. Calabrese, P. Parruccini, and A. I. Sokolov, Phys. Rev. B **68**, 094415 (2003).
[24] G. Zumbach, Phys. Rev. Lett. **71**, 2421 (1993).
[25] G. Zumbach, Nucl. Phys. B **413**, 771 (1994).
[26] G. Zumbach, Phys. Lett. A **190**, 225 (1994).
[27] M. Tissier, B. Delamotte, and D. Mouhanna, Phys. Rev. Lett. **84**, 5208 (2000).
[28] M. Tissier, D. Mouhanna, and B. Delamotte, Phys. Rev. B **61**, 15327 (2000).
[29] M.Tissier, B. Delamotte, and D. Mouhanna, Int. J. Mod. Phys. A **16**, 2131 (2001).
[30] M. Tissier, B. Delamotte, and D. Mouhanna, Phys. Rev. B **67**, 134422 (2003).
[31] B. Delamotte, Yu. Holovatch, D. Ivaneyko, D. Mouhanna and M. Tissier, J. Stat. Mech. **55**, 03014 (2008).
[32] B. Delamotte, M. Dudka, Yu. Holovatch and D. Mouhanna, Phys. Rev. B **82**, 104432 (2010).
[33] B. Delamotte, M. Dudka, Yu. Holovatch and D. Mouhanna, Condens. Matter Phys. **13**, 43703:1 (2010).
[34] F. Kos, D. Poland, D. Simmons-Duffin, and A. Vichi, arXiv:1504.07997 .
[35] Y. Nakayama and T. Ohtsuki, Phys. Rev. D **89**, 126009 (2014).
[36] Y. Nakayama and T. Ohtsuki, Phys. Rev. D **91**, 021901 (2015).
[37] S. El-Showk, M. F. Paulos, D. Poland, S. Rychkov, D. Simmons-Duffin, and A. Vichi, Phys. Rev. D **86**, 025022 (2012).
[38] S. El-Showk, M. F. Paulos, D. Poland, S. Rychkov, D. Simmons-Duffin, and A. Vichi, J. Stat. Phys. **157**, 869 (2014).
[39] C. Wetterich, Nucl. Phys. B **352**, 529 (1991).
[40] C. Wetterich, Z. Phys. C **60**, 461 (1993).
[41] D. F. Litim, Nucl. Phys. B **631**, 128 (2002).
[42] J. Berges, N. Tetradis, and C. Wetterich, Phys. Rep. **363**, 223 (2002).
[43] J. Pawlowski, Annals Phys. **322**, 2831 (2007).
[44] P. Kopietz and L. Bartosch and F. Schtz, *Introduction to the Functional Renormalization Group* (Springer, Berlin, 2010).
[45] O. Rosten, Phys. Rep. **511**, 177 (2012).
[46] S. Nagy, Annals Phys. **350**, 310 (2014).
[47] C. Wetterich, Phys. Lett. B **301**, 90 (1993).
[48] U. Ellwanger, Z. Phys. C **58**, 619 (1993).
[49] N. Tetradis and C. Wetterich, Nucl. Phys. B [FS] **422**, 541 (1994).
[50] T. R. Morris, Int. J. Mod. Phys. A **9**, 2411 (1994).
[51] J.-P. Blaizot, R. Méndez-Galain, and N. Wschebor, Phys. Lett. B **632**, 571 (2006).
[52] J.-P. Blaizot, R. Méndez-Galain, and N. Wschebor, Phys. Rev. E **74**, 051116 (2006).
[53] J.-P. Blaizot, R. Méndez-Galain, and N. Wschebor, Phys. Rev. E **74**, 051117 (2006).
[54] T. R. Morris and M. D. Turner, Nucl. Phys. B **509**, 637 (1998).
[55] L. Canet, B. Delamotte, D. Mouhanna, and J. Vidal, Phys. Rev. B **68**, 064421 (2003).
[56] P. Azaria, B. Delamotte, and T. Jolicoeur, Phys. Rev. Lett. **64**, 3175 (1990).
[57] L. Canet, B. Delamotte, D. Mouhanna, and J. Vidal, Phys. Rev. D **67**, 065004 (2003).
[58] D. Loison, A. I. Sokolov, B. Delamotte, S. A. Antonenko, K. D. Schotte, and H. T. Diep, JETP Lett. **72**, 337 (2000).
[59] S. Yabunaka, B. Delamotte and D. Mouhanna, unpublished, 2015 .